



ELSEVIER

Contents lists available at ScienceDirect

JSES International

journal homepage: [www.jseinternational.org](http://www.jseinternational.org)

## Load-to-failure characteristics of patellar tendon allograft superior capsule reconstruction compared with the native superior capsule

Seth M. Boydstun, MD<sup>a</sup>, Gregory J. Adamson, MD<sup>a,\*</sup>, Michelle H. McGarry, MS<sup>a</sup>,  
James E. Tibone, MD<sup>b</sup>, Thay Q. Lee, PhD<sup>a</sup>

<sup>a</sup>Orthopaedic Biomechanics Laboratory, Congress Medical Foundation, Pasadena, CA, USA

<sup>b</sup>Department of Orthopaedic Surgery, Keck School of Medicine of University of Southern California, Los Angeles, CA, USA

### ARTICLE INFO

#### Keywords:

Superior capsule reconstruction  
Patella tendon allograft  
Native superior capsule  
Structural properties  
Massive rotator cuff tear

Level of evidence: Basic Science Study;  
Biomechanics

**Background:** The potential use of a patellar tendon allograft for superior capsular reconstruction has been demonstrated biomechanically; however, there are concerns regarding compromised fixation strength owing to the longitudinal orientation of the fibers in the patellar tendon. Therefore, the purpose of this study was to compare the fixation strength of superior capsule reconstruction using a patellar tendon allograft to the intact superior capsule.

**Methods:** The structural properties of the intact native superior capsule (NSC) followed by superior capsular reconstruction using a patellar tendon allograft (PT-SCR) were tested in eight cadaveric specimens. The scapula and humerus were potted and mounted onto an Instron testing machine in 20 degrees of glenohumeral abduction. Humeral rotation was set to achieve uniform loading across the reconstruction. Specimens were preloaded to 10 N followed by cyclic loading from 10 N to 50 N for 30 cycles, then load to failure at a rate of 60 mm/min. Video digitizing software was used to quantify the regional deformation characteristics.

**Results:** During cyclic loading, there was no difference found in stiffness between PT-SCR and NSC (cycle 1 – PT-SCR:  $12.9 \pm 3.6$  N/mm vs. NSC:  $22.5 \pm 1.6$  N/mm;  $P = .055$  and cycle 30 – PT-SCR:  $27.3 \pm 1.4$  N/mm vs. NSC:  $25.4 \pm 1.7$  N/mm;  $P = .510$ ). Displacement at the yield load was not significantly different between the two groups (PT-SCR:  $7.0 \pm 1.0$  mm vs. NSC:  $6.5 \pm 0.3$  mm;  $P = .636$ ); however, at the ultimate load, there was a difference in displacement (PT-SCR:  $20.7 \pm 1.1$  mm vs. NSC:  $8.1 \pm 0.5$  mm;  $P < .001$ ). There was a significant difference at both the yield load (PT-SCR:  $71.4 \pm 2.2$  N vs. NSC:  $331.6 \pm 56.6$  N;  $P = .004$ ) and the ultimate load (PT-SCR:  $217.1 \pm 26.9$  N vs. NSC:  $397.7 \pm 62.4$  N;  $P = .019$ ). At the yield load, there was a difference found in the energy absorbed (PT-SCR:  $84.4 \pm 8.9$  N-mm vs. NSC:  $722.6 \pm 156.8$  N-mm;  $P = .005$ ), but no difference in energy absorbed was found at the ultimate load.

**Conclusions:** PT-SCR resulted in similar stiffness to NSC at lower loads, yield displacement, and energy absorbed to ultimate load. The ultimate load of the PT-SCR was approximately 54% of the NSC, which is comparable with the percent of the ultimate load in rotator cuff repair and the intact supraspinatus at time zero.

© 2021 Published by Elsevier Inc. on behalf of American Shoulder and Elbow Surgeons. This is an open access article under the CC BY-NC-ND license (<http://creativecommons.org/licenses/by-nc-nd/4.0/>).

The superior capsule of the glenohumeral joint is a distinct anatomic structure that is essential for function and classified as a passive soft stabilizer of the shoulder.<sup>1,9</sup> In shoulders with massive irreparable rotator cuff tears, the superior capsule is disrupted and the checkrein function of the passive soft-tissue stabilizer is absent.

Investigations were performed at Orthopaedic Biomechanics Laboratory, Congress Medical Foundation, Pasadena, CA, USA. Institutional review board approval was waived by our institution for this basic science study.

\* Corresponding author: Gregory J. Adamson, MD, Congress Medical Foundation, 800 South Raymond Ave, Pasadena, CA 91105, USA.

E-mail address: [cagjamd@aol.com](mailto:cagjamd@aol.com) (G.J. Adamson).

<https://doi.org/10.1016/j.jseint.2021.04.013>

2666-6383/© 2021 Published by Elsevier Inc. on behalf of American Shoulder and Elbow Surgeons. This is an open access article under the CC BY-NC-ND license (<http://creativecommons.org/licenses/by-nc-nd/4.0/>).

This results in increased superior translation of the humerus compromising the abduction capability of the shoulder.<sup>24,25,29</sup>

Superior capsule reconstruction (SCR) was first introduced by Mihata et al<sup>24</sup> in 2012 using a fascia lata autograft to treat irreparable massive rotator cuff tears. These authors first demonstrated the effectiveness of the SCR in biomechanical studies which were followed by clinical studies with outcomes up to five years after surgery.<sup>21,22,24</sup> Specifically, SCR depresses the humeral head and restores the superior stability of the shoulder as well as the deltoid function. A variety of graft sources have been proposed for SCR. Initially, Mihata et al<sup>21,22,24</sup> used a tensor fascia lata (TFL) autograft that is folded over to reach 6- to 8-mm thickness. While supported with clinical outcomes,<sup>21</sup> the harvest of the TFL autograft is

associated with increased donor site morbidity and is difficult to perform if the patient is positioned beach chair. In the United States, human dermal allograft has been used extensively for SCR because of its handling characteristics, strength, and inherent convenience of allograft application.<sup>2</sup> While functional outcomes have been encouraging, healing of the dermal allograft has been variable.<sup>3,6,14,15</sup>

Since the introduction of SCR with TFL autograft, many new graft options have been proposed to avoid donor site morbidity, with the human dermal allograft being the most popular graft currently used for SCR. However, some of the challenges with the human dermal allograft are the thickness of the graft which is typically 3 mm or less and that the human dermal allograft is more flexible and has lower stiffness than that of the TFL. Mihata et al<sup>20,23</sup> showed that thicker fascia lata autograft SCR resulted in lower subacromial contact pressure and decreased superior translation than thinner FL grafts and human dermal allografts. Other autograft options include using the biceps tendon in a looped manner<sup>7</sup> or “snake” configuration.<sup>11</sup> In addition, hamstring autografts have been reported as being used for SCR<sup>28</sup>; however, this comes with obvious donor site morbidity. Patellar tendon,<sup>5</sup> folded TFL<sup>34</sup> and Achilles allografts<sup>13</sup> have also been introduced as an option for graft source. Of these, the patellar tendon allograft has structural characteristics that are advantageous; however, patella tendon grafts have relatively parallel fibers as opposed to a random fiber orientation. A previous biomechanical study showed favorable results using a patellar tendon allograft for SCR,<sup>5</sup> but there are some concerns over a potential risk of decreased fixation strength owing to the predominantly parallel fibers in the patellar tendon. Although the understanding of the importance of the superior capsule is growing, little is known about its function and biomechanical properties. Because the goal of SCR is to recreate the biomechanical function of the superior capsule, the load-to-failure properties of the native superior capsule (NSC) were evaluated and compared with the superior capsular reconstruction using a patellar tendon allograft (PT-SCR). Therefore, the purpose of this study was to quantify the fixation strength of the PT-SCR and compare with the intact NSC in cadaver shoulders without rotator cuff pathology.

## Materials and methods

### *Specimen preparation and testing setup*

Eight nonmatched fresh frozen cadaveric shoulders (mean age  $62.4 \pm 7.7$  years, 6 men and 2 women) were used. The specimens were thawed overnight before dissection. The specimens were completely stripped of skin, soft tissue, and muscle except for the superior glenohumeral joint capsule. All specimens were kept moist with normal saline during dissection and testing to prevent tissue desiccation. During dissection, the specimens were examined to determine if there was any evidence of underlying rotator cuff disease or any other gross abnormalities. One specimen had a complete supraspinatus rotator cuff tear including the superior capsule, so the native capsule could not be tested leaving 7 specimens (mean age  $61.1 \pm 7.4$  years, 5 men and 2 women) for the native vs. PT-SCR analysis with 8 specimens remaining for comparison of PT-SCR fixation displacement. The humerus was transected 8 cm distal to the inferior articular surface of the humeral head.

### *Experimental conditions*

The following two experimental conditions were tested: intact NSC and PT-SCR.

### *Intact superior capsule*

To prepare the NSC, the supraspinatus was reflected from the fossa of the scapula to expose the capsule. The supraspinatus and infraspinatus were then bluntly dissected from the capsule as far laterally as possible to the tuberosity and then transected. The anterior border was sharply defined medial to lateral just posterior to the coracohumeral ligament. The posterior border of the superior capsule was defined as 30 mm posterior to the anterior border. The biceps was then carefully removed from the undersurface of the superior capsule. The labrum was then transected at the anterior and posterior borders on the glenoid. Using a digital caliper and area micrometer, the anterior-to-posterior widths and thickness of the superior capsule were measured at the medial, middle, and lateral aspects.

After preparation and careful dissection of the superior capsule, the specimen was tested in the manner as described in the following text. Once the capsule was loaded to failure, the remaining capsule was sharply transected from the cadaver to leave room for the PT-SCR (Fig. 1, A and B).

### *PT-SCR technique*

Eight patellar tendon grafts from 6 donors (mean age  $46.3 \pm 24.1$  years, 5 men and 1 woman) were used for PT-SCR. The grafts were obtained from JRF Ortho (Centennial, CO, USA) and Community Tissue Services (Dayton, OH, USA) and were irradiated with low-dose gamma 10.5 kGy. To prepare the patellar tendon allograft, bone was removed with a burr from the tibial tubercle to create a 1-cm-wide and 1-mm-thick enthesis. To determine the length of the patellar tendon graft, the medial-to-lateral distance between the glenoid anchors and the medial humeral row anchors with the specimen in 20° abduction was measured. Fifteen millimeters was then added to this measurement to allow for 5 mm medial and 10 mm lateral overlap from the anchor location (Fig. 2). Using a digital caliper and area micrometer, the anterior-to-posterior widths and thickness of the patellar tendon allograft were measured at the medial, middle, and lateral aspects before implantation.

The tibial bone enthesis was placed on the glenoid side for PT-SCR. On the glenoid, fixation was performed using three 3.9-mm Knotless Corkscrew PT anchors (Arthrex, Naples, FL, USA) (Fig. 2). For the humerus, a double-row transosseous-equivalent technique was performed (see Figs. 3 and 4). For the medial row, two 5.5-mm biocomposite Corkscrew FT anchors (Arthrex, Naples, FL, USA) with SutureTape (Arthrex, Naples, FL, USA) were used. For the lateral row, two 4.75-mm biocomposite SwiveLock anchors (Arthrex, Naples, FL, USA) were used.

According to Schon et al,<sup>31</sup> the first glenoid anchor was inserted 5 mm medial to the glenoid face at the 12 o'clock position. The second and third anchors were placed at the 2 o'clock and 10 o'clock positions, respectively, in the same manner at the appropriate angles to ensure adequate anchor fixation within the bone. The first medial-row humerus anchor was placed 5 mm posterior to the posterior edge of the bicipital groove right at the humeral head articular margin. The second anchor was placed 15 mm posterior to the first anchor at the articular margin. The specimen was placed at 20 degrees of glenohumeral abduction. The distance between the glenoid anchors, the anteroposterior distance of the medial row humerus anchors, the mediolateral distance between the anterior glenoid anchor and the anterior medial row humerus anchor, and the mediolateral distance from posterior glenoid anchor to posterior medial row humerus anchor were measured.

The suture limbs of the glenoid knotless suture anchors were passed through the graft in a mattress configuration at the middle

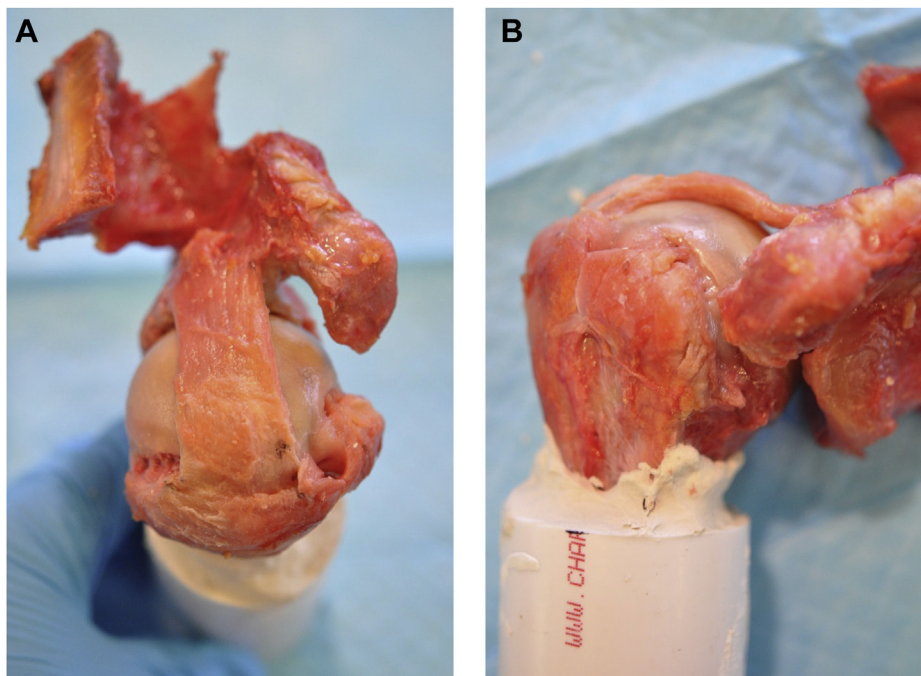


**Figure 1** Native superior capsule after dissection (A) superior view and (B) anterior view.

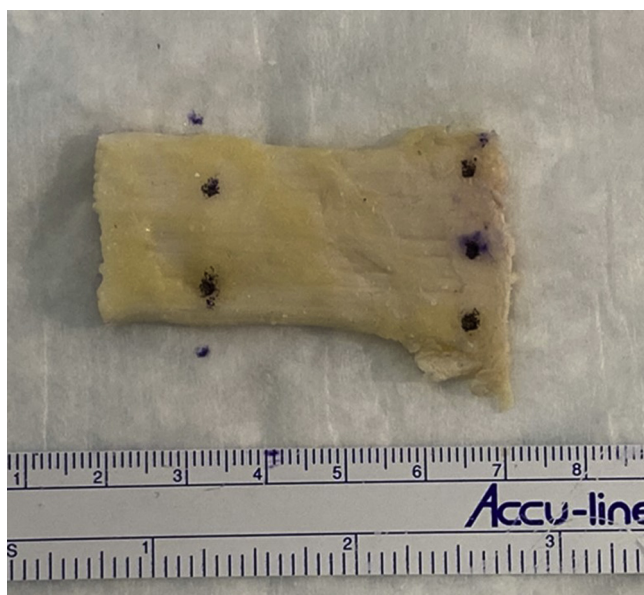


**Figure 2** Patellar tendon allograft after preparation.

of the enthesis at the anterior, middle, and posterior portions corresponding to the location of the glenoid anchor. The sutures were then passed through the looped end of the shuttle suture and pulled through the locking mechanism of the anchor. The graft was then cinched down to the glenoid using a Knot Pusher (Athrex, Naples, FL, USA) for counterforce. The SutureTape of the medial row humerus anchors was passed through the lateral aspect of the graft in a horizontal mattress fashion at predefined points and were tied with a surgeon’s knot with 3 reversing half-hitches on alternating post knots. Once the glenoid and the medial row humerus anchor sutures were passed and knots were tied, the suture limbs from the humerus anchors were placed in a transosseous-equivalent fashion

into the 2 SwiveLock anchors 1 cm lateral to the lateral edge of the graft in line with the respective medial row anchors.

*Biomechanical testing*

The scapula was potted in a metal box with the glenoid parallel to the face of the box and the humerus was potted in 1.5-inch PVC pipe with plaster of paris. Specimens were then mounted onto an Instron material testing machine in 20 degrees of glenohumeral abduction (Fig. 3, A and B). Humeral rotation was set such that visually equal tension was placed on both the anterior and posterior borders of the native capsule or SCR. Acrylic paint was used to mark the anterior and posterior borders of the specimen for video digitizing analysis of deformation. Specimens were then preloaded with 10 N followed by cyclic loading from 10 N to 50 N for 30 cycles, then loaded to failure at a rate of 60 mm/min. A testing protocol similar to rotator cuff repair protocols performed in our laboratory was used. The peak cyclic load was chosen to be lower than the yield load of the PT-SCR construct based on pilot studies performed. Thirty cycles were chosen as the amount of creep and hysteresis by this number of cycles had stabilized.<sup>26</sup> WINAnalyze software was used to digitally track the markers for measuring displacement. This displacement was then matched with the Instron load to generate the load-displacement curve. Displacement with cyclic loading, yield load, yield displacement, ultimate load, ultimate displacement, and energy absorbed to failure were analyzed. The modes of failure were also recorded.

*Statistics*

Data were averaged for the eight specimens, and the standard error was calculated. All data are presented as mean ± standard error. Statistical analysis was performed using a paired t-test with a  $P < .05$  to represent statistical differences.

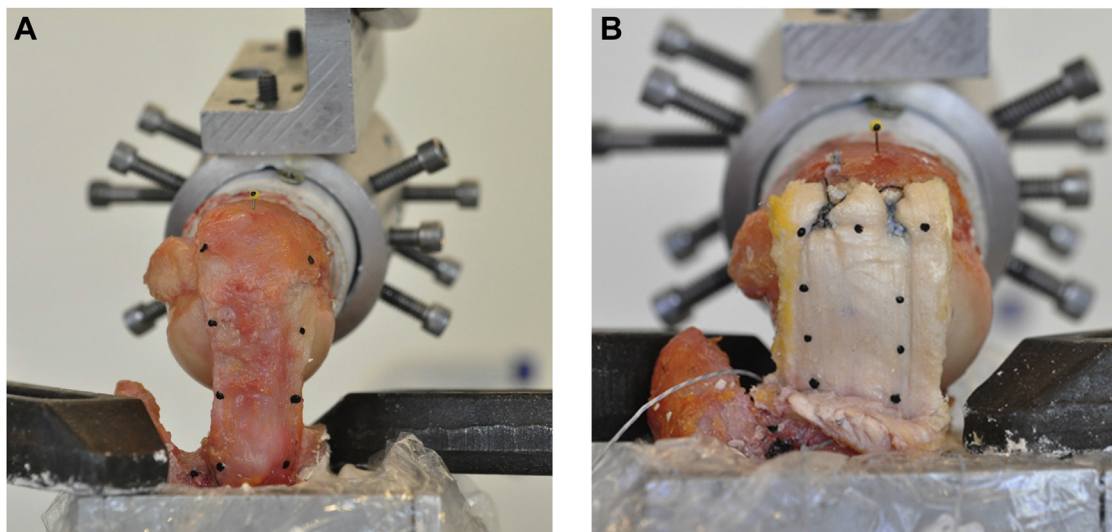


**Figure 3** Photograph of a specimen mounted on the Instron material testing machine for (A) native superior capsule and (B) after patella tendon superior capsule reconstruction.

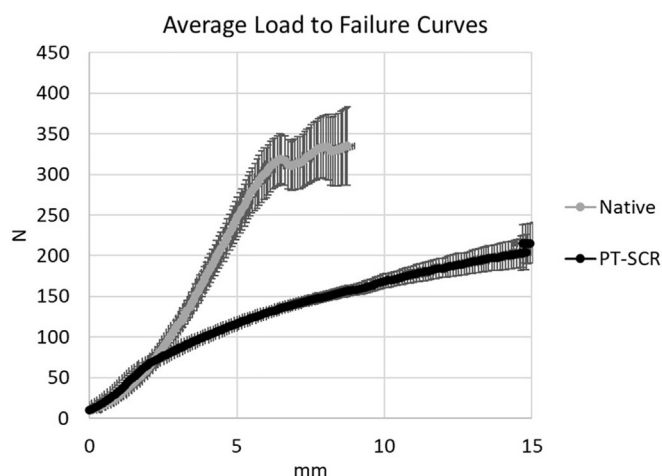


**Figure 4** The average load-to-failure curves for both the native superior capsules and after patella tendon superior capsule reconstruction. Note the displacement data from the cyclic loading were subtracted from the start value to start both curves at zero displacement. PT-SCR, superior capsular reconstruction using a patellar tendon allograft.

## Results

### Specimens

The NSC average thickness was  $2.4 \pm 0.1$  mm which was significantly less than the thickness of the PT-SCR which was  $5.3 \pm 0.5$  mm ( $P = .002$ ). There was no significant difference in the average length of the NSC ( $54.5 \pm 1.5$  mm) compared with the average length of the PT-SCR ( $52.1 \pm 0.8$  mm) ( $P = .2$ ); however, the width of the NCS ( $26.2 \pm 1.0$  mm) was significantly smaller than that of the PT-SCR ( $32.5 \pm 0.7$  mm) ( $P = .001$ ).

### Modes of failure

The NSC modes of failure were as follows: medial + lateral (1), midsubstance (2), lateral (3), and medial only (1). The PT-SCR

modes of failure were as follows: lateral and medial suture slip (8), lateral suture cut through (8), medial suture cut through (2), and medial anchor pullout (1).

### Cyclic loading

All load-to-failure characteristics are presented in [Table I](#).

During cyclic loading, there was no difference found in stiffness between PT-SCR and NSC (at cycle 1 – PT-SCR:  $12.9 \pm 3.6$  N/mm vs. NSC:  $22.5 \pm 1.6$  N/mm;  $P = .055$  and at cycle 30 – PT-SCR:  $27.3 \pm 1.4$  N/mm vs. NSC:  $25.4 \pm 1.7$  N/mm;  $P = .510$ ). Conversely, there was a difference found with hysteresis between the two groups, at both cycle 1 and cycle 30 (at cycle 1 – PT-SCR:  $78.4 \pm 13.9$  N-mm vs. NSC:  $8.3 \pm 1.4$  N-mm;  $P = .002$  and at Cycle 30 – PT-SCR:  $5.9 \pm 0.9$  N-mm vs. NSC:  $3.0 \pm 0.5$  N-mm;  $P = .014$ ).

### Load to failure

The average load-to-failure curves for both groups are shown in [Figure 4](#). During load to failure of the specimens, the linear stiffness of the NSC was significantly greater than that of the PT-SCR ( $84.0 \pm 13.7$  N/mm vs.  $30.4 \pm 1.3$  N/mm;  $P = .009$ ). Displacement at the yield load was not significantly different between the two groups (PT-SCR:  $7.0 \pm 1.0$  mm vs. NSC:  $6.5 \pm 0.3$  mm;  $P = .636$ ); however, at the ultimate load, there was a difference in displacement (PT-SCR:  $20.7 \pm 1.1$  mm vs. NSC:  $8.1 \pm 0.5$  mm;  $P < .001$ ). There was a significant difference at both the yield load (PT-SCR:  $71.4 \pm 2.2$  N vs. NSC:  $331.6 \pm 56.6$  N;  $P = .004$ ) and the ultimate load (PT-SCR:  $217.1 \pm 26.9$  N vs. NSC:  $397.7 \pm 62.4$  N;  $P = .019$ ). At the yield load, there was a difference found in the energy absorbed (PT-SCR:  $84.4 \pm 8.9$  N-mm vs. NSC:  $722.6 \pm 156.8$  N-mm;  $P = .005$ ), but no difference in the energy absorbed was found at the ultimate load (PT-SCR:  $2350.6 \pm 437.8$  N-mm vs. NSC:  $1317.1 \pm 283.3$  N-mm;  $P = .080$ ).

### PT-SCR fixation displacement

There were no significant differences between medial and lateral PT-SCR fixation displacement for cyclic loading or load to failure ([Fig. 5](#)).

**Table 1**  
Cyclic loading and load-to-failure characteristics of the native superior capsule and after patella tendon superior capsule reconstruction.

Biomechanical parameter	Native superior capsule	Patella tendon SCR	P value
<b>Cyclic loading</b>			
Linear stiffness (N-mm)			
Cycle 1	22.5 ± 1.6	12.9 ± 3.6	.055
Cycle 30	25.4 ± 1.7	27.3 ± 1.4	.510
Hysteresis (N-mm)			
Cycle 1	8.3 ± 1.4	78.4 ± 13.9	.002
Cycle 30	3.0 ± 0.5	5.9 ± 0.9	.014
<b>Load to failure</b>			
Linear stiffness (N-mm)	84.0 ± 13.7	30.4 ± 1.3	.009
Yield load (N)	331.6 ± 56.6	71.4 ± 2.2	.004
Yield displacement (mm)	6.5 ± 0.3	7.0 ± 1.0	.636
Energy absorbed to yield (N-mm)	772.6 ± 156.8	84.4 ± 8.9	.005
Ultimate load (N)	397.7 ± 62.4	217.1 ± 26.9	.019
Ultimate displacement (mm)	8.1 ± 0.5	20.7 ± 1.1	<.001
Energy absorbed to ultimate (N-mm)	1317.1 ± 283.3	2350.6 ± 437.8	.080

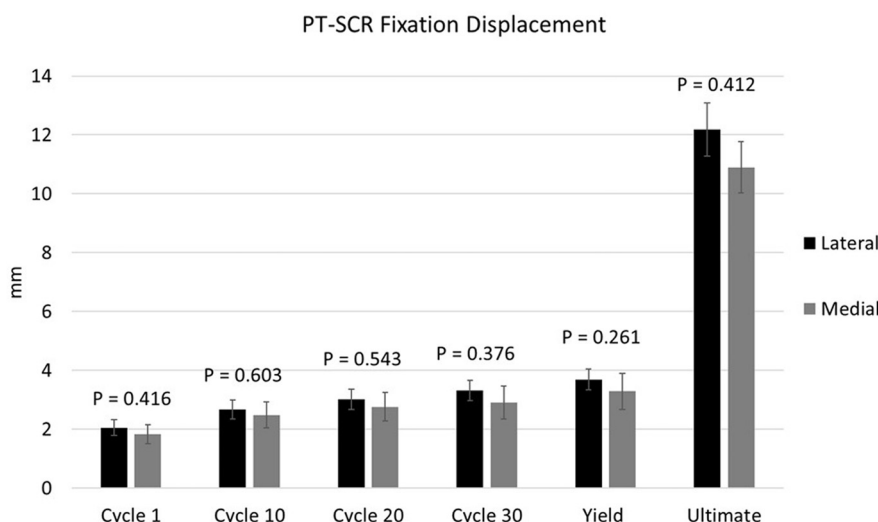


**Figure 5** Medial and lateral fixation displacement after patella tendon SCR (PT-SCR). PT-SCR, superior capsular reconstruction using a patellar tendon allograft.

**Discussion**

One of the biggest findings from the present study was that there was no difference in the stiffness during cyclic loading. Hysteresis was larger for PT-SCR vs. the NSC for cycle 1, most likely owing to elongation of the fixation of the graft-suture/anchor interface. By cycle 30, the hysteresis for the PT-SCR had decreased by 92%. In addition, there was no difference in displacement at the yield load or the energy absorbed at the ultimate load even though yield and ultimate loads were higher for the NSC. These loads occurred at displacement values greater than those that would represent clinical failure.

With the introduction of the SCR by Mihata et al<sup>24</sup> in 2012, shoulder surgeons now have a more viable treatment option for irreparable rotator cuff tears in younger patients who do not have advanced arthritis. Recently, Mihata et al<sup>21</sup> showed favorable five year outcomes for patients who had SCR with a fascia lata autograft. This treatment option is a much more viable option than reverse total shoulder arthroplasty for younger patients with this shoulder pathology. While the results for SCR by Mihata et al<sup>21</sup> were achieved with a fascia lata autograft, there are some concerns of donor site morbidity.

While the original graft choice was a fascia lata autograft, there are many other options that exist. One commonly used allograft for

SCR is an acellular human dermal graft.<sup>2,6,8,32</sup> One issue is that this graft is typically thinner than the originally described fascia lata autograft.<sup>21,22,24</sup> Mihata et al<sup>23</sup> previously showed that thicker fascia lata autografts had lower subacromial contact pressure and superior translation than thinner grafts. With the intent of using a thicker graft and prevent autograft harvesting complications, the patellar tendon has also been described.<sup>5</sup> These grafts are thicker than the typically acellular human dermal allograft.

SCR failure is as high as 65% in some articles when using acellular dermal allograft.<sup>35</sup> Woodmass et al<sup>35</sup> showed that the failure rate was 44% at the 1-year follow-up and 64% at the 2-year follow-up. Despite an initial increase in acromiohumeral distance at the 2-week follow-up, Denard et al<sup>6</sup> showed no improvement in the acromiohumeral distance at the final follow-up with healing rates of 45%.

One previous study evaluated the elongation of a dermal allograft with and without suture reinforcement during cyclic loading from 10 N to 100 N.<sup>16</sup> From this study, the native dermal graft stiffness for cycle 1 was 17.69 N/mm and 25.72 N/mm for cycle 30, which corresponds with the PT-SCR in this study at cycle 30. This was a saw bone model that sought to only evaluate the graft tissue, not the entire repair construct, and they did not test load to failure. The authors also reported an increase in graft length and decrease in thickness with cyclic loading.<sup>16</sup> In addition, the dermal allograft

has been shown to elongate by approximately 15% and decrease in thickness by approximately 20% after rotational range of motion and kinematic testing.<sup>20</sup> Conversely, a fascia lata allograft<sup>20</sup> and patellar tendon allograft<sup>5</sup> demonstrated minimal deformation. The patellar tendon has a Young's modulus and ultimate strain that is more comparable with fascia lata than to a dermal allograft.<sup>4,5</sup> The results of the present study also showed deformation characteristics similar to the inferior glenohumeral ligament.<sup>18,19</sup>

Tendon repairs are never as strong as their native tissues. The tensile strength of the native supraspinatus tendon has been reported to be from 652 N to 1114 N in cadaveric studies<sup>10,17,27</sup> with two of these authors evaluating different regions of the tendon reporting that the anterior portion alone has a tensile strength greater than 400 N.<sup>10,17</sup> With the invention of rotator cuff repair anchors, rotator cuff repair has evolved from transosseous bone tunnels to single-row, double-row, and transosseous equivalent repair. The time-zero repair strength of transosseous repairs, single-row repairs, and all suture anchor repairs has been reported to be around 300N<sup>12,30,33</sup>; whereas double row repairs and transosseous equivalent repairs have been reported as high as 500N.<sup>12,26,30</sup> Using a midrange of tensile strength from the literature for the native cuff (870 N), these percentages range from 34% to 57%. The ultimate load of the PT-SCR was approximately 54% of the NSC which is comparable with the percent of the ultimate load in rotator cuff repair and the intact supraspinatus at time zero.

The present study has some limitations. The most obvious limitation of the present study is the time-zero nature that is found in all biomechanical studies. While the superior capsule was reconstructed using a patellar tendon allograft, this cadaveric model did not account for graft healing. In addition, only the NSC and PT-SCR were tested without the presence of any other static and dynamic stabilizers around the shoulder. Without other tissues present, this could have altered how the graft behaves in a clinical setting. This study also fails to biomechanically compare different graft options when performing SCR. Because the goal of the SCR is to recreate the biomechanical function of the superior capsule, the load-to-failure properties of the NSC were evaluated and compared with PT-SCR. Future studies are planned for further comparison of PT-SCR with other graft materials.

## Conclusion

PT-SCR resulted in similar stiffness to NSC at lower loads, yield displacement, and the energy absorbed to the ultimate load. The ultimate load of the PT-SCR was approximately 54% of the NSC, which is comparable with the percent of the ultimate load in rotator cuff repair and the intact supraspinatus at time zero.

## Disclaimers:

**Funding:** Partial funding was provided by Congress Medical Foundation. Arthrex Inc (Naples, FL, USA) donated anchors used; JRF Ortho (Centennial, CO, USA) and Community Tissue Services (Dayton, OH, USA) donated cadaveric specimens and Patella Tendon Allografts.

**Conflicts of interest:** Gregory J. Adamson received research support from Arthrex, Inc. for projects other than this study. Thay Q. Lee is a paid consultant and received research support from Arthrex, Inc. for projects other than this study. The other authors, their immediate family, and any research foundation with which they are affiliated have not received any financial payments or other benefits from any commercial entity related to the subject of this article.

## Acknowledgments

The authors would like to thank the following for support of this project: Congress Medical Foundation for partial funding; Arthrex, Inc (Naples, FL, USA) for donating anchors used; JRF Ortho (Centennial, CO, USA) and Community Tissue Services (Dayton, OH, USA) for donating cadaveric specimens and Patella Tendon Allografts.

## References

- Adams CR, DeMartino AM, Rego G, Denard PJ, Burkhart SS. The rotator cuff and the superior capsule: Why We need both. *Arthroscopy* 2016;32:2628-37. <https://doi.org/10.1016/j.arthro.2016.08.011>.
- Burkhart SS, Denard PJ, Adams CR, Brady PC, Hartzler RU. Arthroscopic superior capsular reconstruction for massive irreparable rotator cuff repair. *Arthrosc Tech* 2016;5:e1407-18. <https://doi.org/10.1016/j.eats.2016.08.024>.
- Burkhart SS, Prancun JJ, Hartzler RU. Superior capsular reconstruction for the Operatively irreparable rotator cuff tear: clinical outcomes are Maintained 2 Years after surgery. *Arthroscopy* 2020;36:373-80. <https://doi.org/10.1016/j.arthro.2019.08.035>.
- Butler DL, Grood ES, Noyes FR, Zernicke RF, Brackett K. Effects of structure and strain measurement technique on the material properties of young human tendons and fascia. *J Biomech* 1984;17:579-96.
- Croom WP, Adamson GJ, Lin CC, Patel NA, Kantor A, McGarry MH, et al. A biomechanical cadaveric study of patellar tendon allograft as an alternative graft material for superior capsule reconstruction. *J Shoulder Elbow Surg* 2019;28:1241-8. <https://doi.org/10.1016/j.jse.2018.12.015>.
- Denard PJ, Brady PC, Adams CR, Tokish JM, Burkhart SS. Preliminary results of arthroscopic superior capsule reconstruction with dermal allograft. *Arthroscopy* 2018;34:93-9. <https://doi.org/10.1016/j.arthro.2017.08.265>.
- El-shaar R, Sooin S, Nicandri G, Maloney M, Voloshin I. Superior capsular reconstruction with a Long head of the biceps tendon autograft: a cadaveric study. *Orthop J Sport Med* 2018;6. <https://doi.org/10.1177/2325967118785365>.
- Hirahara AM, Adams CR. Arthroscopic superior capsular reconstruction for treatment of massive irreparable rotator cuff tears. *Arthrosc Tech* 2015;4:e637-41. <https://doi.org/10.1016/j.eats.2015.07.006>.
- Ishihara Y, Mihata T, Tamboli M, Nguyen L, Park KJ, McGarry MH, et al. Role of the superior shoulder capsule in passive stability of the glenohumeral joint. *J Shoulder Elbow Surg* 2014;23:642-8. <https://doi.org/10.1016/j.jse.2013.09.025>.
- Itoi E, Berglund LJ, Grabowski JJ, Schultz FM, Growney ES, Morrey BF, et al. Tensile properties of the supraspinatus tendon. *J Orthop Res* 1995;13:578-84.
- Kim D, Jang Y, Park J, On M. Arthroscopic superior capsular reconstruction with biceps autograft: snake technique. *Arthrosc Tech* 2019;8:e1085-92. <https://doi.org/10.1016/j.eats.2019.05.023>.
- Kim DH, ElAttrache NS, Tibone JE, Jun BJ, DeLaMora SN, Kvitne RS, et al. Biomechanical comparison of a single-row versus double-row suture anchor technique for rotator cuff repair. *Am J Sports Med* 2006;34:407-14. <https://doi.org/10.1177/0363546505281238>.
- Kim JW, Nam DJ. Arthroscopic superior capsular reconstruction by the Mini-Open Modified Keyhole technique using an Achilles tendon–bone allograft. *Arthrosc Tech* 2020;9:e275-81. <https://doi.org/10.1016/j.eats.2019.10.007>.
- Lacheta L, Horan MP, Schairer WW, Goldenberg BT, Dornan GJ, Pogorzelski J, et al. Clinical and Imaging outcomes after arthroscopic superior capsule reconstruction with human dermal allograft for irreparable Posterosuperior rotator cuff tears: a Minimum 2-year follow-up. *Arthroscopy* 2020;36:1011-9. <https://doi.org/10.1016/j.arthro.2019.12.024>.
- Lacheta L, Millett PJ. Editorial Commentary: superior capsule reconstruction using dermal allograft in Posterosuperior rotator cuff tears—do patients benefit and allografts heal? *Arthroscopy* 2020;36:381-2. <https://doi.org/10.1016/j.arthro.2019.11.103>.
- Lee CS, Reddy M, Scott B, Curtis D, Amirouche F, Athviraham A. Suture Tape–Reinforced human dermal allograft used for superior capsule reconstruction Demonstrates improved Ability to Withstand elongation. *Arthrosc Sport Med Rehabil* 2020;2:e511-5. <https://doi.org/10.1016/j.asmr.2020.05.015>.
- Matsushashi T, Hooke AW, Zhao KD, Goto A, Sperling JW, Steinmann SP, et al. Tensile properties of a morphologically split supraspinatus tendon. *Clin Anat* 2014;27:702-6. <https://doi.org/10.1002/ca.22322>.
- McMahon PJ, Dettling J, Sandusky MD, Tibone JE, Lee TQ. The anterior band of the inferior glenohumeral ligament. Assessment of its permanent deformation and the anatomy of its glenoid attachment. *J Bone Joint Surg Br* 1999;81:406-13.
- McMahon PJ, Dettling JR, Sandusky MD, Lee TQ. Deformation and strain characteristics along the length of the anterior band of the inferior glenohumeral ligament. *J Shoulder Elbow Surg* 2001;10:482-8.

20. Mihata T, Bui CNH, Akeda M, Cavagnaro MA, Kuenzler M, Peterson AB, et al. A biomechanical cadaveric study comparing superior capsule reconstruction using fascia lata allograft with human dermal allograft for irreparable rotator cuff tear. *J Shoulder Elbow Surg* 2017;26:2158-66. <https://doi.org/10.1016/j.jse.2017.07.019>.
21. Mihata T, Lee TQ, Hasegawa A, Fukunishi K, Kawakami T, Fujisawa Y, et al. Five-year follow-up of arthroscopic superior capsule reconstruction for irreparable rotator cuff tears. *J Bone Joint Surg Am* 2019;101:1921-30. <https://doi.org/10.2106/JBJS.19.00135>.
22. Mihata T, Lee TQ, Watanabe C, Fukunishi K, Ohue M, Tsujimura T, et al. Clinical results of arthroscopic superior capsule reconstruction for irreparable rotator cuff tears. *Arthroscopy* 2013;29:459-70. <https://doi.org/10.1016/j.arthro.2012.10.022>.
23. Mihata T, McGarry MH, Kahn T, Goldberg I, Neo M, Lee TQ. Biomechanical Effect of thickness and tension of fascia lata graft on glenohumeral stability for superior capsule reconstruction in irreparable supraspinatus tears. *Arthroscopy* 2016;32:418-26. <https://doi.org/10.1016/j.arthro.2015.08.024>.
24. Mihata T, McGarry MH, Pirolo JM, Kinoshita M, Lee TQ. Superior capsule reconstruction to restore superior stability in irreparable rotator cuff tears: a biomechanical cadaveric study. *Am J Sports Med* 2012;40:2248-55. <https://doi.org/10.1177/0363546512456195>.
25. Oh JH, Jun BJ, McGarry MH, Lee TQ. Does a critical rotator cuff tear stage exist? A biomechanical study of rotator cuff tear progression in human cadaver shoulders. *J Bone Jt Surg - Ser A* 2011;93:2100-9. <https://doi.org/10.2106/JBJS.J.00032>.
26. Park MC, Tibone JE, ElAttrache NS, Ahmad CS, Jun BJ, Lee TQ. Part II: biomechanical assessment for a footprint-restoring transosseous-equivalent rotator cuff repair technique compared with a double-row repair technique. *J Shoulder Elbow Surg* 2007;16:469-76. <https://doi.org/10.1016/j.jse.2006.09.011>.
27. Rickert M, Georgousis H, Witzel U. [Tensile strength of the tendon of the supraspinatus muscle in the human. A biomechanical study]. *Unfallchirurg* 1998;101:265-70.
28. Rosales-Varo AP, Zafra M, García-Espona MA, Flores-Ruiz MA, Roda O. Superior capsular reconstruction of irreparable rotator cuff tear using autologous hamstring graft. *Rev Esp Cir Ortop Traumatol* 2019;63:1-6. <https://doi.org/10.1016/j.recot.2018.08.004>.
29. Rybalko D, Bobko A, Amirouche F, Peresada D, Hussain A, Patetta M, et al. Biomechanical effects of superior capsular reconstruction in a rotator cuff-deficient shoulder: a cadaveric study. *J Shoulder Elbow Surg* 2020;29:1959-66. <https://doi.org/10.1016/j.jse.2020.03.007>.
30. Salata MJ, Sherman SL, Lin EC, Sershon RA, Gupta A, Shewman E, et al. Biomechanical evaluation of transosseous rotator cuff repair: do anchors really matter? *Am J Sports Med* 2013;41:283-90. <https://doi.org/10.1177/0363546512469092>.
31. Schon JM, Katthagen JC, Dupre CN, Mitchell JJ, Turnbull TL, Adams CR, et al. Quantitative and Computed Tomography anatomic analysis of glenoid fixation for superior capsule reconstruction: a cadaveric study. *Arthroscopy* 2017;33:1131-7. <https://doi.org/10.1016/j.arthro.2016.10.016>.
32. Tokish JM, Beicker C. Superior capsule reconstruction technique using an acellular dermal allograft. *Arthrosc Tech* 2015;4:e833-9. <https://doi.org/10.1016/j.eats.2015.08.005>.
33. Trofa DP, Ruder JA, Yeatts NC, Peindl RD, Habet NA, Saltzman BM, et al. Cyclic and load-to-failure properties of all-suture anchors in human cadaveric shoulder greater Tuberosities. *Arthroscopy* 2020;36:2805-11. <https://doi.org/10.1016/j.arthro.2020.06.010>.
34. Vredenburgh ZD, Prodrromo JP, Tibone JE, Dunphy TR, Weber J, McGarry MH, et al. Biomechanics of tensor fascia lata allograft for superior capsular reconstruction. *J Shoulder Elbow Surg* 2020;30:178-87. <https://doi.org/10.1016/j.jse.2020.04.025>.
35. Woodmass JM, Wagner ER, Borque KA, Chang MJ, Welp KM, Warner JJP. Superior capsule reconstruction using dermal allograft: early outcomes and survival. *J Shoulder Elbow Surg* 2019;28:S100-9. <https://doi.org/10.1016/j.jse.2019.04.011>.